

## Disruption Database Studies for ITER

T.C. Hender<sup>1</sup>, J.C. Wesley<sup>2</sup>, P.C. de Vries<sup>1</sup>, S.M. Flanagan<sup>2</sup>, E.D. Fredrickson<sup>3</sup>, D.A. Gates<sup>3</sup>, R.S. Granetz<sup>4</sup>, Y. Gribov<sup>5</sup>, D.F. Howell<sup>1</sup>, A.W. Hyatt<sup>2</sup>, M.F. Johnson<sup>1</sup>, Y. Kawano<sup>6</sup>, J.B. Lister<sup>7</sup>, R. Martin<sup>1</sup>, J.E. Menard<sup>3</sup>, G. Pautasso<sup>8</sup>, D.P. Schissel<sup>2</sup>, E.J. Strait<sup>2</sup>, and M. Sugihara<sup>5</sup>

1) Euratom/UKAEA Fusion Association, Culham Science Centre, Abingdon OX14 3DB, UK

2) General Atomics, P.O. Box 85608, San Diego, California 92186-5608, USA

3) Princeton Plasma Physics Laboratory, Princeton, New Jersey, USA

4) Plasma Science Fusion Center, MIT, Cambridge Massachusetts, USA

5) ITER Organization, Cadarache Centre, 13108 St Paul lez Durance, France

6) JAEA, Fusion Research and Development Directorate, Naka, Ibaraki, Japan

7) Association Euratom-Confederation Suisse, CRPP, EPFL, Lausanne, Switzerland

8) Max Planck Institut für Plasmaphysik, Euratom Association, Garching, Germany

### Introduction

Data on the expected characteristics of disruptions and on the nature and magnitude of disruption effects are needed for the design and functional validation of ITER components and systems. A new International Disruption Database (IDDB) [1] has been established by the International Tokamak Physics Activity (ITPA) Topical Group on MHD, Disruption and Magnetic Control. Version 1 of the database, hosted by General Atomics, now comprises device attributes and data from a total of 3875 discharges that end in disruption or some similar type of fast plasma-current terminating event (e.g. a vertical displacement event (VDE) or a massive gas injection (MGI) fast plasma shutdown). The present content represents submissions from eight devices: Alcator C-Mod (2167), ASDEX Upgrade (51), DIII-D (1153), JET (200), JT-60U (20), MAST (55), NSTX (200) and TCV (29). The data cover the ranges of major radius  $0.54 \leq R(m) \leq 3.19$  and plasma current  $0.08 \leq I_p(MA) \leq 3.42$ , as shown in figure 1, and an aspect ratio range of  $1.27 \leq R/a \leq 6.62$ . The examples with  $R/a > 4.09$  arise from a small number of reduced-minor-radius examples contained within the DIII-D data. With these data excepted, the effective

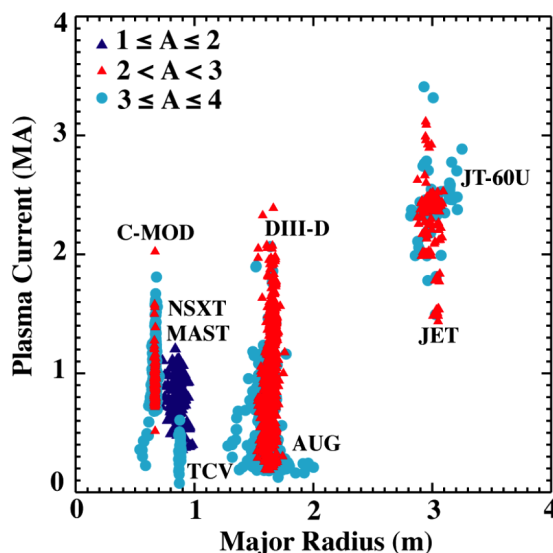


Fig. 1 Ranges of plasma current, major radius and aspect ratio ( $A$ ) encompassed by the IDDB data.

range of aspect ratio for the collective v.1 data set is  $1.27 \leq R/a \leq \sim 4.1$ . Data content of v.1 comprises some 70 scalar variables that quantify the contributing device and device-specific configuration attributes, before-disruption plasma current, shape and other disruption-relevant magnetic and kinetic attributes, plus detailed data on the rate and waveform characteristics of the plasma current decay.

### Current quench rates

The first application of the database has been in determining the fastest  $I_p$  quench rate, which is important in calculating the loading on ITER blanket modules [2]. For this study the current quench (CQ) time is defined as

$$t_{CQ} = 5/3 \Delta t_{60} = 5/3 (t_{20} - t_{80}) \quad (1)$$

where  $t_{80}$  and  $t_{20}$  are respectively the times for the plasma current to decay, after disruption onset, to 80% and 20% of the initial before-disruption plasma current,  $I_{p0}$ . In contrast to the previous *ad hoc* current quench database content used for [2,3], the v.1 contributed data now uniformly comprise directly-measured  $t_{80}$  and  $t_{20}$  values. It should be noted that although the current quench time is linearly extrapolated from the 80-20% quench time, there is no presumption the decay is of that form (see [2] for a discussion on this issue). Figure 2 shows the quench times of the v.1 data normalized by the plasma area ( $S$ ) versus the current density, defined as  $j_p = I_{p0}/S$ . The basis for normalising the current decay time ( $t_{CQ}$ ) by  $S$  is discussed in [3] and the data are plotted versus  $j_p$  (as in the *IPB* [3]) as a convenient way to display data from a range of tokamaks and to connect present data to the range of current densities expected in ITER (the pink-shaded domain indicated in figure 2). The NSTX and MAST data clearly have faster  $I_p$ -quench rates than the conventional  $R/a$  tokamaks. The lower bound for the low aspect ratio data is  $t_{CQ}/S \geq 0.6 \text{ ms/m}^2$ , about 3 times lower than the bound for the standard aspect ratio data. However, figure 3 shows that when the area-normalized CQ times for all of the v.1 tokamaks are further normalized by their respective dimensionless self-inductance factors,  $L^* = \ln(8R/a) - 1.75$ , the low aspect ratio data now approximately overlays the similar- $j_p$  data from the other standard aspect ratio tokamaks. We caution that the accuracy of our present inductance renormalization procedure is not sufficient to support fine-scale distinctions between the minimum renormalized current quench times for low versus conventional aspect ratio tokamaks.

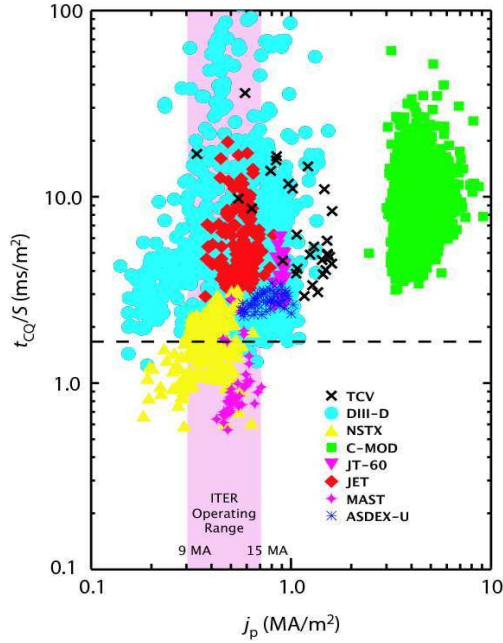


Fig. 2. Area normalized CQ rate versus current density

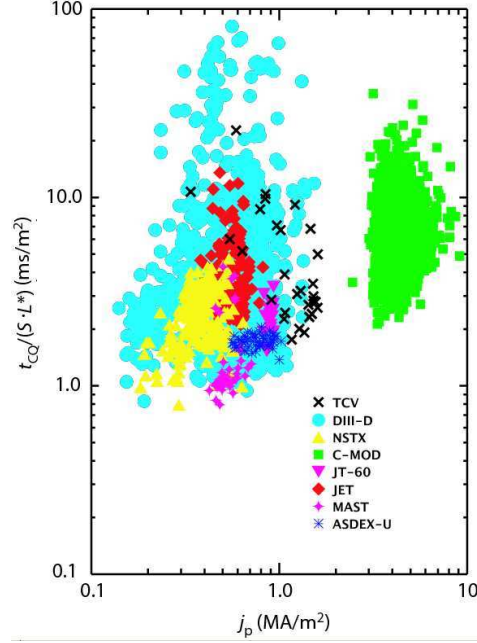


Fig. 3. Area and inductance normalized CQ rate versus current density

Neglecting for the moment the NSTX and MAST data, we see from figure 2 that the DIII-D data has the fastest area-normalized CQs of the six standard-aspect-ratio tokamaks represented. In figure 4, we show a high-resolution plot of the fastest  $S$ -normalized DIII-D current quenches versus  $1/q_{cyl}$  ( $=I_p(\text{MA})R(\text{m})/[5a^2(\text{m})B_t(\text{T})]$ ); the nominal ITER value of  $1/q_{cyl}=0.88$ , which corresponds to  $q_{95}=3$  (ITER scenario 2). Figure 4 shows a reasonably clear division of the data; around, and above the nominal ITER  $1/q_{cyl}$ -value all data lie at or above  $t_{CQ}/S = 1.67 \text{ ms/m}^2$ . However, there are twelve data points (out of a total of 1153) with  $t_{CQ}/S < 1.67 \text{ ms/m}^2$ , at higher  $q_{cyl}$  values. The risk the fastest CQs pose to ITER is due to the CQ-induced rapid flux change at the first wall structure. For a given CQ rate, the larger the plasma current, the larger the induced voltage, so risk scales with the plasma current (or as  $1/q_{cyl}$ ) and inversely with the CQ rate. Hence the diagonal line in figure 4 represents a line of equal risk from a disruption at a given toroidal field. Points above the diagonal line represent a reduced risk, compared to a disruption with  $t_{CQ}/S = 1.67 \text{ ms/m}^2$  at full nominal current ( $I_p=15\text{MA}$ ) in ITER. Thus the points with  $t_{CQ}/S < 1.67 \text{ ms/m}^2$  do not need to be accounted for in considering the fastest CQ in ITER. This is the basis for choosing  $t_{CQ}/S=1.7\text{ms/m}^2$  (to 2 significant figures) as the recommended fastest CQ rate ( $t_{\min} \cong 36 \text{ ms}$  for  $S = 21.3 \text{ m}^2$  in ITER). It should be noted that for the other two large v.1 IDDB datasets, from JET and C-Mod, the area-normalized lower bound is approximately  $3.0 \text{ ms/m}^2$ ; whereas the lower

bounds for ASDEX Upgrade and JT-60U are  $\sim 2.4 \text{ ms/m}^2$ . We can find no simple explanation internal to the IDDB data as to why the DIII-D lower bound is noticeably lower than that of the other standard aspect ratio tokamaks. Also it should be noted that the database shows a large spread in CQ times, with the majority lying well above the fastest observed value of  $t_{CQ}/S$  – for example in DIII-D just 4.9% of the data has a quench time faster than  $2 \text{ ms/m}^2$ .

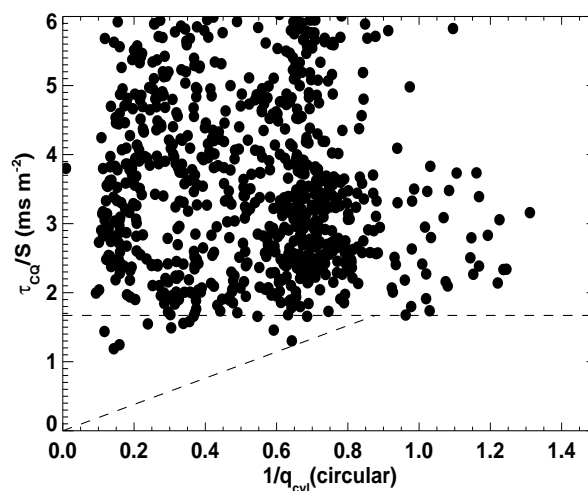


Fig 4 DIII-D data for  $t_{CQ}/S$  versus  $1/q_{\text{cyl}}$ . The diagonal line represents a line of equal disruption induced current at a given toroidal field.

The discussion of CQ rates has been based on a linear extrapolation from 80 to 20% quench times. Extrapolations based on other %-intervals (starting from a maximum of 90% and going to a minimum of 10%) have also been explored and with a very limited number of exceptions the bound  $t_{CQ}/S > 1.7 \text{ ms/m}^2$  is obeyed. Further an exponential fit to the  $I_p$  data (at 8 times during the decay) shows a lower CQ time bound that is very consistent with an exponential fit to the 80 and 20% data points.

### Future Plans

Near-term future plans for the IDDB call for expansion of the v.1 data set to include detailed time-dependent pre-disruption waveforms to allow pre-disruptive energy loss to be assessed. Also initial data on halo currents will be included. On a longer time scale, we anticipate further expansion of the IDDB data set to encompass thermal quench and plasma-facing-component energy deposition and comprehensive runaway electron related data.

### References

- [1] J C Wesley et al, 2006 IAEA Fusion Energy Conf (Chengdu, China), paper IT/P1-21
- [2] M Sugihara, IAEA FEC 2004 paper IT-P3/-29.
- [3] ITER Physics Basis, Chapter 3, Nucl Fus **39** (1999) 2251.

*This work was supported in part by the UK Engineering and Physical Sciences Research Council, by the European Communities under the contract of Association between EURATOM and UKAEA, and in part by the U.S. Department of Energy under DE-FC02-04ER54698 and DE-AC02-76CH03073. The views and opinions expressed herein do not necessarily reflect those of the European Commission.*